Proposal for a Tunable and Switchable Multiwavelength Laser With Variable Spacing Based on Broadband Cascaded Quadratic Nonlinearity

Gang Qu, Yuping Chen, Mingjun Gong, and Xianfeng Chen

***Abstract*—A scheme to realize a tunable and switchable multi-wavelength laser with variable wavelength spacing is proposed based on broadband cascaded quadratic nonlinear interactions in an aperiodically poled MgO-doped lithium niobate (MgO:APPLN) waveguide. Four output wavelengths can be generated simultaneously from the laser and can be switched by tuning the operation temperature of MgO:APPLN. Additionally, the four output wavelengths of the laser can be selected by launching two seeded lights with different wavelengths and wavelength spacing. This device, capable of wavelength tunable function, will facilitate applications in the fiber sensing and wavelength routing for dense wavelength-division-multiplexed (WDM) networks.**

***Index Terms*—Cascaded quadratic nonlinearity, multiwavelength laser, optical frequency conversion.**

I. Introduction

MULTIWAVELENGTH laser sources have potential applications in dense wavelength-division-multiplexed (WDM) systems, optical instrument testing and characterization, optical fiber sensors, and spectroscopy, and such light sources are particularly in-demand in optical communication because they provide an efficient and economical solution to increase the flexibility of WDM systems [1]. Though some kinds of tunable multiwavelength lasers have been proposed and developed including multiple distributed-feedback (DFB) lasers [2], multiwavelength Raman lasers [3], four-wave-mixing (FWM) effect by utilizing high nonlinear fiber such as photonic crystal fibers (PCFs) [4], [5], and dispersion shifted fibers (DSFs) [6], etc, the output wavelengths of these multiwavelength lasers are not conveniently tunable, which limits their flexibility and functionality in applications.

Manuscript received September 08, 2009; revised December 27, 2009. Current version published March 10, 2010. This work was supported by the National High Technology Research and Development Program (863) of China (No. 2007AA01Z273), the National Natural Science Fund of China (10874120 and 60407006), and sponsored by the Scientific Research Foundation for the Returned Overseas Chinese Scholars, State Education Ministry.

The authors are with the State Key Laboratory of Advanced Optical Communication System and Networks, Department of Physics, Shanghai Jiao Tong University, 200240 Shanghai, China (e-mail: ypchen@sjtu.edu.cn; xfchen@sjtu.edu.cn).

Color versions of one or more of the figures in this paper are available online at http://ieeexplore.ieee.org.

Digital Object Identifier 10.1109/JQE.2010.2041431

It is well known that, with the quasi-phase-matching (QPM) technique, it is possible to realize expected wavelength conversion with relatively high efficiency [7], [8]. Effective QPM-based wavelength conversions have been demonstrated with periodically poled $LiNbO_3$. However, one distinct drawback of this kind of wavelength converter is that the QPM-wavelength and temperature tolerances are very small [9], [10]. One solution to this problem is using an aperiodic optical superlattices (AOS) structure which can supply much more reciprocal vectors for multiple QPM than that of periodically poled crystals, and it has been employed to achieve multiple and broadband QPM process [11]. Therefore, the cascaded nonlinear process, with the broadband second-harmonic generation (SHG) [12] and difference-frequency generation (DFG) [13] in AOS, is a novel and effective way to realize the multiwavelength conversion. In our previous work, we have reported a flexible multi-wavelength conversion experimentally in periodically poled MgO-doped lithium niobate (MgO:PPLN) [14], which is based on another type I broadband QPM by employing the intrinsic dispersion of MgO doped lithium niobate (MgO:LN) and polarization control of input lights [15], [16]. The possible candidate way to construct a multiwavelength laser is to use QPM cascaded second-order interaction in lithium niobate waveguide, which can present an ultrafast response, potentially low switching power, wide wavelength coverage and integration compatibility with fiber communication system [17], [18].

In this paper, based on our previous theoretical [13] and experimental results [14], a novel scheme to realize a tunable and switchable multiwavelength laser in an aperiodically poled 5-mol% MgO-doped lithium niobate (MgO:APPLN) waveguide is proposed, which is implemented by the cascaded second-harmonic generation and difference-frequency generation (cSHG/DFG) process at room temperature. The wavelengths and the wavelength spacings of the output waves can be tunable by changing the wavelengths and their spacing of the two input pumps. In addition, the proposed multiwavelength laser is also switchable via changing the operation temperature, which could be beneficial to the flexibility of WDM fiber network.

II. Basic Principle Operation

Fig. 1 shows the schematic diagram of the tunable multiwavelength laser in the MgO:APPLN waveguide. The insert is

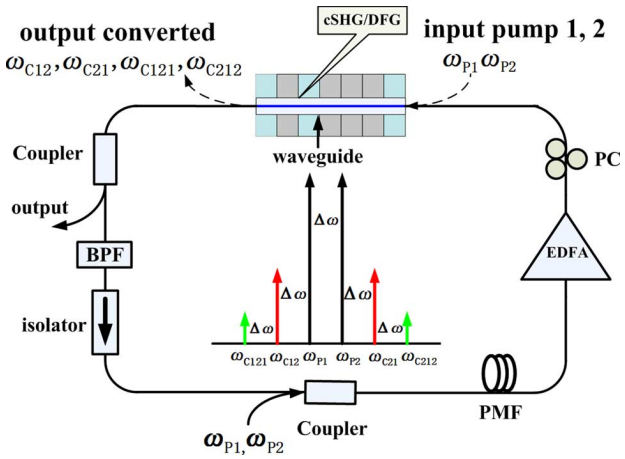

Fig. 1. Schematic diagram of the tunable multiwavelength laser in MgO:APPLN waveguide. EDFA, erbium-doped fiber amplifier; PMF, polarization-maintaining fiber; PC, polarization controller; BPF, bandpass filter.

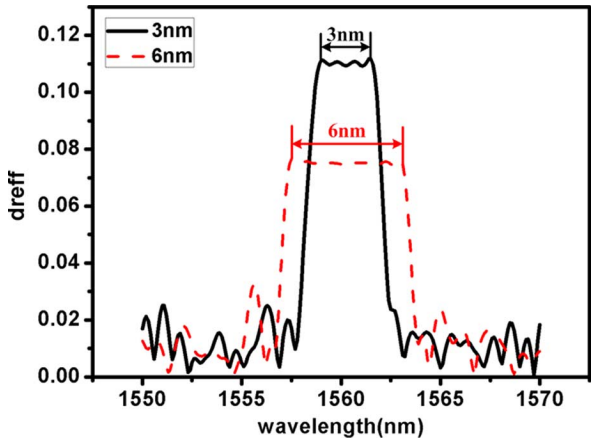

Fig. 2. Comparison of effective quadratic nonlinearity called d_{reff} with different flattop bandwidths of 3 nm and 6 nm.

an illustration of the two pumps and the converted waves with the same angular frequency spacing $\Delta\omega$, ω_{P1} and ω_{P2} denote pump waves, and ω_{C12}, ω_{C21}, ω_{C121} and ω_{C212} represent converted waves. Here, we employ the quadratic cascading nonlinear wavelength conversion in MgO:APPLN to generate new wavelengths. This multiwavelength laser consists of a MgO:APPLN waveguide as main device, two couplers, a polarization controller, an EDFA as light power amplification, PMFs, an isolator and a bandpass filter. The PC inserted after the EDFA is to ensure the two input pumps as extraordinary lights. The input pumps P1 and P2 participate in the cSHG/DFG nonlinear interactions and generate new converted waves C12, C21, C121 and C212 (the meanings of the number signs will be explained in part III). The pump sources as seed lights are two strong pumps at the 1.55 μm in the configuration, which cannot be used as pump for erbium-doped fiber (EDF). The waveguide sample is divided into layers with the same thickness L_0 which is less than the coherence length of the DFG process. The positive and negative signs in each layer stand for the poling orientations of QPM, corresponding to the signs of nonlinear optical coefficient. The total length of $LiNbO_3$ sample in our proposed device is 19.8 mm, and it is divided into 6600 layers with the same thickness 3 μm of each layer. The irregular poling orientation of each layer, corresponding to the sign of nonlinear optical coefficient, can be determined through the simulated annealing (SA) method when we select an appropriate object function. And this aperiodical domain-inverted structure can provide desirable reciprocal lattice vectors for multiple QPM than that of periodically poled crystals to meet the expected phase matching conditions, and it has been employed to achieve multiple and broadband QPM process. [19], [20].

In the design, the flattop bandwidth of SHG QPM is significant, which decides the numbers of output wavelengths and their output powers. After specified calculation through choosing the optical arrangement carefully, we can obtain the prescribed broaden flattop bandwidth as shown in Fig. 2. Since the pump and second-harmonic waves are all extraordinary waves, the SHG process utilizes the largest component of the nonlinear coefficient tensor d_{33}. Then we use (1):

$$d_{\text{reff}} = \frac{d_{\text{eff}}}{d_{33}} \tag{1}$$

to calculate the conversion efficiency, where d_{reff} refers to the reduction in effective nonlinearity comparing with that for the perfect phase-match process[13], [21].

We design two AOS QPM structures and give their comparison. We find that, there is a tradeoff between the conversion efficiency and the flattop bandwidth in designing this device. The comparison of d_{reff} with different flattop bandwidths is shown in Fig. 2.

The solid line and dashed line represent the 3 nm and 6 nm flattop bandwidths with same central wavelength 1560.25 nm, respectively. Obviously, if d_{reff} is bigger, the flattop bandwidth is smaller. The maximal d_{reff} is about 0.112 with pre-designed for 3 nm flattop bandwidth at 21 °C. While the pre-designed flattop bandwidth is 6 nm, the maximal d_{reff} approximately decreases to 0.075, which corresponds to lower conversion efficiency.

III. The Quadratic Cascading Nonlinear Process

In the quadratic cascading nonlinear process of cSHG/DFG, when the pump beam P1 (ω_{P1}) propagating along the MgO:APPLN waveguide, a second-harmonic wave SH1 (ω_{SH1}) is yielded with the frequency doubled ($\omega_{SH1} = 2\omega_{P1}$) through the SHG process. In the subsequent DFG process, pump beam P2 (ω_{P2}) interacts with the second-harmonic wave SH1 (ω_{SH1}) to generate a converted wave C12 ($\omega_{C12} = 2\omega_{P1} - \omega_{P2}$). Here, C12 denotes the cSHG/DFG process of $\omega_{SH1} = 2\omega_{P1}$, $\omega_{C12} = \omega_{SH1} - \omega_{P2}$. Hereafter, C21 represents the process of $\omega_{SH2} = 2\omega_{P2}$, $\omega_{C21} = \omega_{SH2} - \omega_{P1}$; C121 denotes the process of $\omega_{SH1} = 2\omega_{P1}$, $\omega_{C121} = \omega_{SH1} - \omega_{C21}$ and C212 denotes the process of $\omega_{SH2} = 2\omega_{P2}$, $\omega_{C212} = \omega_{SH2} - \omega_{C12}$.

In the following discussions, we assume that the optical waves propagate as a single waveguide mode along z axis in the MgO:APPLN waveguide. The propagation loss is neglected since it does not qualitatively change the response of the device except for reducing the amplitude of the field distribution. It is noticed that the second-harmonic waves generated by the converted waves C12 and C21 are neglected since the two input pump powers are much higher than the powers of the C21 and C12. For simplicity, we take the generation of converted wave C12 as an example to illustrate the nonlinear process and calculation in the following discussion.

A. Coupled Equations

Under the slowly varying envelope approximation and nondepletion approximation during the cSHG/DFG processes, the cSHG/DFG processes can be modeled by a set of simplified coupled equations.

$$\frac{\partial A_{P1}}{\partial z} = i\omega_{P1}\kappa_{SHG1}A_{P1}^{*}A_{SH1}\exp(i\Delta k_{SHG1}z) \quad (2a)$$

$$\frac{\partial A_{SH1}}{\partial z} = \frac{i}{2}\omega_{SH1}\kappa_{SHG1}A_{P1}A_{P1}\exp(-i\Delta k_{SHG1}z) \quad (2b)$$

$$\frac{\partial A_{P2}}{\partial z} = i\omega_{P2}\kappa_{DFG1}A_{C12}^{*}A_{SH1}\exp(i\Delta k_{DFG1}z) \quad (3a)$$

$$\frac{\partial A_{C12}}{\partial z} = i\omega_{C12}\kappa_{DFG1}A_{P2}^{*}A_{SH1}\exp(i\Delta k_{DFG1}z) \quad (3b)$$

where A_l, λ_l and P_l represent, respectively, the field distribution, wavelength and power at ω_l. The subscripts denote the pump P1, pump P2, second-harmonic wave SH1 and converted wave C12, respectively. The refractive indexes of different extraordinary optical waves n_l can be given by Sellmeier equations [22].

Δk_{SHG1} and Δk_{DFG1} represent the phase mismatch for the SHG process and DFG process, respectively. And κ_{SHG1} is the SHG coupling coefficient given by

$$\kappa_{SHG1} = d_{\text{reff}} \cdot d_{33}\sqrt{\frac{2\mu_0}{cn_{P1}^2 n_{SH1}A_{\text{eff}}}} \quad (4)$$

where κ_{DFG1} is the DFG coupling coefficient given by

$$\kappa_{DFG1} = d_{\text{reff}} \cdot d_{33}\sqrt{\frac{2\mu_0}{cn_{P2}n_{C12}n_{SH1}A_{\text{eff}}}}. \quad (5)$$

μ_0 is the permeability of free space, A_{eff} is the effective nonlinear interaction area, and c denotes the light velocity in vacuum.

B. Analytical Solutions

To gain insight into the device operation, the small-signal approximation is employed, in which $P_{P1}(z)$ and $P_{P2}(z)$ are assumed to be constant during the interactions. We utilize a similar derivation process [23] to get analytical solutions. When the phase-match conditions of the SHG process are satisfied, the mismatch of wave-vector $\Delta k_{SHG1} = 0$, then the (2b) can be solved as

$$A_{SH1} \approx \frac{i}{2}\omega_{SH1}\kappa_{SHG1}A_{P1}^{2}z. \quad (6)$$

Substituting (6) into (3b), we can derive

$$\begin{aligned} A_{C12} &\approx -\frac{1}{2}\omega_{C12}\omega_{SH1}\kappa_{SHG1}\kappa_{DFG1} \\ &\quad \cdot A_{P1}^{2}A_{P2}^{*}\int_0^L \exp(i\Delta k_{DFG1}z)z\,dz \\ &\quad -\frac{1}{2}\omega_{C12}\omega_{SH1}\kappa_{SHG1}\kappa_{DFG1}A_{P1}^{2}A_{P2}^{*} \\ &\quad \cdot\Big\{\Big[\frac{L}{\Delta k_{DFG1}}\sin(\Delta k_{DFG1}L) + \frac{\cos(\Delta k_{DFG1}L)-1}{\Delta k_{DFG1}^{2}}\Big] \\ &\quad + i\Big[\frac{\sin(\Delta k_{DFG1}L)}{\Delta k^{2}{}_{DFG1}} - \frac{L}{\Delta k_{DFG1}}\cos(\Delta k_{DFG1}L)\Big]\Big\}, \quad (7) \end{aligned}$$

where L is the length of the AOS structure. So, the optical power of converted wave C12 is

$$P_{C12} \approx \frac{1}{4}\omega_{C12}^{2}\omega_{SH1}^{2}\kappa_{SHG1}^{2}\kappa_{DFG1}^{2}P_{P1}^{2}P_{P2}f(\Delta k_{DFG1}, L) \quad (8)$$

and the expression of $f(\Delta k_{DFG1}, L)$ is

$$\begin{aligned} f(\Delta k_{DFG1}, L) &= \frac{L^2}{\Delta k_{DFG1}^{2}}\sin c^{2}\left(\frac{\Delta k_{DFG1}L}{2}\right) \\ &\quad -\frac{2L^2}{\Delta k_{DFG1}^{2}}\sin c(\Delta k_{DFG1}L) + \frac{L^2}{\Delta k_{DFG1}^{2}}. \quad (9) \end{aligned}$$

When the phase-match conditions of the DFG process are satisfied, the mismatch of wave-vector $\Delta k_{DFG1} = 0$, then we can obtain

$$P_{C12} = \frac{L^4}{16}\omega_{C12}^{2}\omega_{SH1}^{2}\kappa_{SHG1}^{2}\kappa_{DFG1}^{2}P_{P1}^{2}P_{P2}. \quad (10)$$

Following the power calculation steps above, we can obtain the other power expressions of the converted waves C21, C121 and C212.

C. Numerical Simulation and Performance of Device

The wavelengths of the converted waves C12 and C121 are calculated by (11) and (12), respectively,

$$\lambda_{C12} = \frac{\lambda_{P1}\lambda_{P2}}{2\lambda_{P2} - \lambda_{P1}} \quad (11)$$

$$\lambda_{C121} = \frac{\lambda_{P1}\lambda_{P2}}{3\lambda_{P2} - 2\lambda_{P1}}. \quad (12)$$

The wavelengths of the converted waves C21 and C212 are calculated by (13) and (14), respectively,

$$\lambda_{C21} = \frac{\lambda_{P1}\lambda_{P2}}{2\lambda_{P1} - \lambda_{P2}} \quad (13)$$

$$\lambda_{C212} = \frac{\lambda_{P1}\lambda_{P2}}{3\lambda_{P1} - 2\lambda_{P2}}. \quad (14)$$

Obviously, from the above (11)–(14)λ_{C12}, λ_{C21}, λ_{C121} and λ_{C212} are tunable through tuning the pump wavelengths λ_{P1} and λ_{P2}.

In our simulation, we adopt the length of each layer $L_0 = 3\,\mu$m, and the number of the layers $N = 6600$, so the total length of the AOS structure L is 19.8 mm. The flattop bandwidth for

3 nm is pre-designed with the central wavelength at 1560.25 nm. The effective nonlinear interaction area is $A_{\text{eff}} = 50\ \mu\text{m}^2$.

Fig. 3 shows the powers of the converted waves and pumps at 21 °C. The input powers of the two pumps are both set at 400 mW. $\Delta\lambda_0$ ($\Delta\lambda_0 = \lambda_{P2} - \lambda_{P1}$) is the wavelength spacing between the two input pumps. The solid lines represent the powers with wavelength spacing $\Delta\lambda_0 = 0.4$ nm, corresponding to the frequency spacing of 50 GHz. The powers of the converted waves for C12, C21, C121 and C212 are -9.37 dBm, -9.38 dBm, -44.77 dBm and -44.77 dBm, respectively. We can see that, even if there is a flattop bandwidth of SHG, the conversion efficiency of cSHG/DFG at different input wavelengths is different when referred from the (10). So the powers of converted waves, such as C12 and C21, produced in the first cSHG/DFG process are much higher than C121 and C212, those produced in the second cSHG/DFG process. The dashed lines represent the powers with $\Delta\lambda_0 = 1.2$ nm, corresponding to the frequency spacing of 150 GHz. The powers of converted waves for C12, C21, C121 and C212 are 9.37 dBm, 9.39 dBm, -56.91 dBm and -44.78 dBm, respectively. Apparently, C121's power declines a lot, because C21 is outside the flattop bandwidth where the value of d_{reff} falls sharply. Table I shows the outputs for different input wavelengths (one input fixed at 1560 nm) with different wavelength spacings of 0.4 nm, 0.8 nm, 1.2 nm and 1.6 nm (the corresponding frequency spacings are 50 GHz, 100 GHz, 150 GHz and 200 GHz, respectively). Assuming no output with the power less than -45 dBm, we use hollow circles to represent them, which stand for "off" states, while solid circles represent effective outputs above -45 dBm, which stand for "on" states. We find that there are 4 outputs when the frequency spacings are 50 GHz and 100 GHz as C12 and C21 are both seated in the flattop bandwidth, and just 3 outputs are "on" with the frequency spacings of 150 GHz as C21 is outside the flattop bandwidth. At frequency spacing of 200 GHz, both C12 and C21 are outside the flattop bandwidth, only 2 outputs are at "on" states. Since the flattop bandwidth is fixed, and the broader the frequency spacings are, the fewer the number of outputs is.

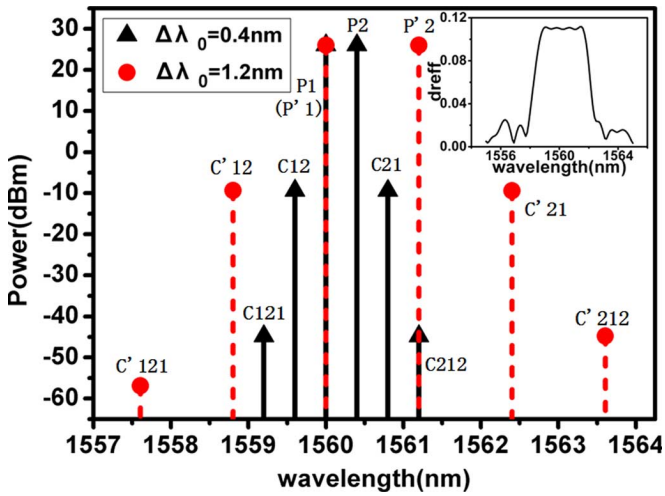

Fig. 3. Powers of the converted waves vs. input pumps with different multi-wavelength spacings of 0.4 nm and 1.2 nm at 21 °C. The insert is the corresponding SHG QPM broadened flattop bandwidth of 3 nm for the inputs of 1555 nm and 1565 nm.

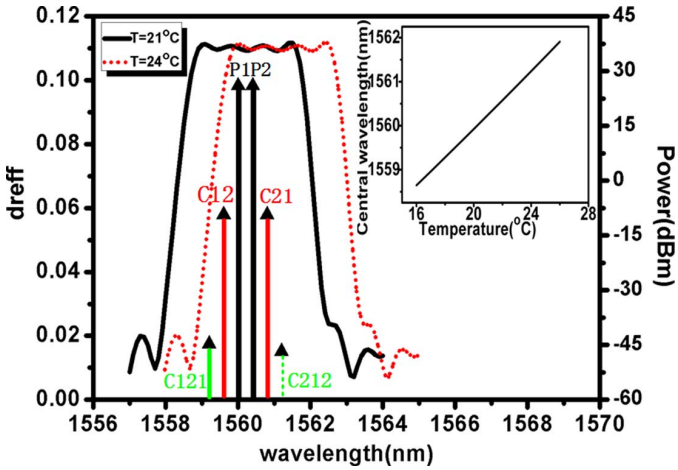

Fig. 4. Switchable performance (C212 is "off" at 24 °C) with shift of broad flattop bandwidth by tuning operation temperature from 21 °C to 24 °C. The insert is the temperature dependency of the central wavelength of the broad bandwidth.

IV. Switchable Performance of Device

With the variation of the operation temperature, the central wavelength of the flattop band in Fig. 2 shifts while the shape of the broadened flattop does not change as illustrated in Fig. 4. The inset in Fig. 4 shows the central wavelength of the broad flattop depends linearly on the operation temperature and the tuning rate of temperature with the central wavelength is about 0.32 nm/°C.

Fig. 4 shows that the proposed multiwavelength laser can be switchable by tuning the temperature from 21°C to 24 °C. Assuming the powers of the converted waves below -45 dBm can be neglected. When the operation temperature is 21 °C, all the output wavelengths locate in the flattop bandwidth, where d_{reff} is the maximal, and all the output waves are at "on" states. With increasing the operation temperature to 24 °C, the central wavelength is shifted to 1561.21 nm, then the outputs C12 and C121 are out of the flattop bandwidth, meanwhile, d_{reff} declines sharply, so the power of the converted wave C212 decreases to -46.82 dBm as C212 is produced from the cSHG/DFG process $\omega_{C212} = 2\omega_{P2} - \omega_{C12}$, and becomes "off" state. Then, 4 simultaneously generated wavelengths at 21 °C fall to 3 only via

TABLE I
The Outputs of Converted Waves With Different Wavelength Spacing From 0.4 nm to 1.6 nm

converted waves	wavelength spacing (nm)			
	0.4(50GHz) (λ_{P2}=1560.4)	0.8(100GHz) (λ_{P2}=1560.8)	1.2(150GHz) (λ_{P2}=1561.2)	1.6(200GHz) (λ_{P2}=1561.6)
12	●	●	●	●
21	●	●	●	●
121	●	●	○	○
212	●	●	●	○

TABLE II
THE "ON" AND "OFF" STATES OF OUTPUT CONVERTED WAVES WITH TEMPERATURE FROM 16 °C TO 26 °C

Converted waves	Temperature (°C)										
	16	17	18	19	20	21	22	23	24	25	26
12	●	●	●	●	●	●	●	●	●	●	●
21	●	●	●	●	●	●	●	●	●	●	●
121	○	○	○	●	●	●	●	●	●	○	○
212	○	○	●	●	●	●	●	●	○	○	○

increasing the operation temperature from 21 °C to 24 °C. Following the above performance, we demonstrate the "on" and "off" states of all converted waves with the temperature variation at the room temperature in Table II. Similar to Table I, the solid circles represent "on" states and the hollow circles mean the corresponding wavelengths are "off" states.

V. CONCLUSION

We have proposed a novel scheme to fulfill a tunable and switchable multiwavelength laser based on the cascading nonlinear process cSHG/DFG in MgO:APPLN waveguide. Analytical expressions are derived and provide an insight into the operation characteristics of this device. 4 tunable wavelengths are generated simultaneously through tuning the wavelengths of the two input pumps in flattop bandwidth. The pre-designed flattop SHG bandwidth of MgO:APPLN can be increased through choosing more appropriate poling orientation of each layer to increase the numbers of multiple wavelength outputs. However, there is a tradeoff between the bandwidth and the conversion efficiency, i.e., the wider is the flattop bandwidth, the smaller is d_{reff}, corresponding to lower conversion efficiency. So we have to design the optimal arrangement of APPLN to balance the numbers of output lasers and their output powers. The wavelength spacings of outputs and their numbers are variable by inputting two seed lights with different wavelength spacing and changing external temperature. If the inputs and the external temperature are stable, then the outputs cannot be changed.

For the cascaded quadratic nonlinear processes are transparent in signal format and high speed response, the proposed device here has other potential multiple practical applications when integrated with its other network functions, such as wavelength conversion and optical delay line in high bit rate WDM networks.

REFERENCES

[1] M. Aljada, K. Alameh, and Y. T. Lee, "A tunable multiwavelength laser employing a semiconductor optical amplifier and an opto-VISI processor," *IEEE Photon. Technol. Lett.*, vol. 20, pp. 815–817, May 2008.

[2] W. Li, W.-P. Huang, X. Li, and J. Hong, "Multiwavelength gain-coupled DFB laser cascade: design modeling and simulation," *IEEE J. Quantum Electron.*, vol. 36, no. 10, pp. 1110–1116, Oct. 2000.

[3] Y.-G. Han, C.-S. Kim, J. U. Kang, U.-C. Paek, and Y. Chung, "Multiwavelength Raman fiber-ring laser based on tunable cascaded long-period fiber gratings," *IEEE Photon. Technol. Lett.*, vol. 15, pp. 383–385, Mar. 2003.

[4] Zhang, H. Liu, M. S. Demokan, and H. Y. Tam, "Stable and broad bandwidth multiwavelength fiber ring laser incorporating a highly nonlinear photonic crystal fiber," *IEEE Photon. Technol. Lett.*, vol. 17, pp. 2535–2537, Dec. 2005.

[5] X. M. Liu, Y. Chung, A. Lin, W. Zhao, K. Q. Lu, Y. S. Wang, and T. Y. Zhang, "Tunable and switchable multi-wavelength erbium-doped fiber laser with highly nonlinear photonic crystal fiber and polarization controllers," *Laser Phys. Lett.*, vol. 5, no. 12, pp. 904–907, Aug. 2008.

[6] Y. G. Han, T. V. A. Tran, and S. B. Lee, "Wavelength-spacing tunable multiwavelength erbium-doped fiber laser based on four-wave mixing of dispersion-shifted fiber," *Opt. Lett.*, vol. 31, no. 6, pp. 697–699, Mar. 2006.

[7] M. H. Chou, I. Brener, M. M. Fejer, E. E. Chaban, and S. B. Christman, "1.5-μm-band wavelength conversion based on cascaded second-order nonlinearity in $LiNbO_3$ waveguides," *IEEE Photon. Technol. Lett.*, vol. 11, pp. 653–655, Jun. 1999.

[8] Y. Fukuchi, M. Akaike, and J. Maeda, "Characteristics of all-optical ultrafast gate switches using cascade of second-harmonic generation and difference frequency mixing in quasi-phase-matched lithium niobate waveguides," *IEEE J. Quantum Electron.*, vol. 41, pp. 729–734, May 2005.

[9] G. Schreiber, H. Suche, Y. L. Lee, W. Grundkotter, V. Quiring, R. Ricken, and W. Sohler, "Efficient cascaded difference frequency conversion in periodically poled Ti: $LiNbO_3$ waveguides using pulsed and CW pumping," *Appl. Phys. B*, vol. 73, pp. 501–504, Aug. 2001.

[10] Y. Chen, R. Wu, X. Zeng, Y. Xia, and X. Chen, "Type I quasi-phase-matched blue second harmonic generation with different polarizations in periodically poled $LiNbO_3$," *Optics and Laser Technol.*, vol. 38, no. 1, pp. 19–22, Feb. 2006.

[11] Y. W. Lee, F. C. Fan, Y. C. Huang, B. Y. Gu, B. Z. Dong, and M. H. Chou, "Nonlinear multiwavelength conversion based on an aperiodic optical superlattice in lithium niobate," *Opt. Lett.*, vol. 27, no. 24, pp. 2191–2193, Dec. 2002.

[12] K. Mizuuchi, K. Yamamoto, M. Kato, and H. Sato, "Broadening of the phase-matching bandwidth in quasi-phase-matched second-harmonic generation," *IEEE J. Quantum Electron.*, vol. 30, pp. 1596–1604, Jul. 1994.

[13] W. Xie, X. Chen, Y. Chen, and Y. Xia, "All-optical variable-in variable-out wavelength converter based on cascaded nonlinearity in aperiodic optical superlattice," *Opt. Commun.*, vol. 251, no. 1, pp. 179–185, Jul. 2005.

[14] J. Zhang, Y. Chen, F. Lu, and X. Chen, "Flexible wavelength conversion via cascaded second order nonlinearity using broadband SHG in MgO-doped PPLN," *Opt. Exp.*, vol. 16, no. 10, pp. 6957–6962, May 2008.

[15] J. Zhang, Y. Chen, F. Lu, W. Lu, W. Dang, X. Chen, and Y. Xia, "Effect of MgO doping of periodically poled lithium niobate on second-harmonic generation of femtosecond laser pulses," *Appl. Opt.*, vol. 46, no. 32, pp. 7792–7796, Nov. 2007.

[16] R. Wu, Y. Chen, J. Zhang, X. Chen, and Y. Xia, "Broadening of the second-harmonic phase-matching bandwidth in type II periodically poled KTP," *Appl. Opt.*, vol. 44, no. 26, pp. 5561–5564, Sep. 2005.

[17] Cristiani, G. P. Banfi, V. Degiorgio, and L. Tartara, "Wavelength shifting of optical pulses through cascaded second-order processes in a lithium-niobate channel waveguide," *Appl. Phys. Lett.*, vol. 75, no. 9, pp. 1198–1200, Aug. 1999.

[18] S. Kawanishi, M. H. Chou, K. Fujiura, M. M. Fejer, and T. Morioka, "All-optical modulation time-division-multiplexing of 100 Gbit/s signal using quasi-phase matched mixing in $LiNbO_3$ waveguides," *Electron. Lett.*, vol. 36, no. 18, pp. 1568–1569, Aug. 2000.

[19] B.-Y. Gu, B.-Z. Dong, Y. Zhang, and G.-Z. Yang, "Enhanced harmonic generation in aperiodic optical superlattices," *Appl. Phys. Lett.*, vol. 75, no. 15, pp. 2175–2177, Oct. 1999.

[20] S. Kirkpatrick, C. D. Gelatt, and M. P. Vecchi, "Optimization by simulated annealing," *Science*, vol. 220, no. 4598, pp. 671–680, May 1983.

[21] B.-Y. Gu, Y. Zhang, and B.-Z. Dong, "Investigations of harmonic generations in aperiodic optical superlattices," *J. Appl. Phys.*, vol. 87, no. 11, pp. 7629–7637, Feb. 2000.

[22] D. Zelmon, D. Small, and D. Jundt, "Infrared corrected sellmeier coefficients for congruently grown lithium niobate and 5 mol. magnesium oxide doped lithium niobate," *J. Opt. Soc. Am. B*, vol. 14, no. 12, pp. 3319–3322, Dec. 1997.

[23] J. Wang, J. Sun, X. Zhang, and D. Huang, "All-optical tunable wavelength conversion with extinction ratio enhancement using periodically poled lithium niobate waveguides," *J. Lightw. Technol.*, vol. 26, no. 17, pp. 3137–3148, Sep. 2008.

Gang Qu was born in Hubei province, China, on June 14, 1984. He received the B.S. degree in electronic information engineering from Huazhong University of Science and Technology (HUST), Wuhan, China, in 2008. He is currently working toward the M.S. degree at the department of Physics, Shanghai Jiao Tong University (SJTU), Shanghai, China.

He is currently with the State Key Laboratory of Advanced Optical Communication System and Networks, SJTU. His research interests include all-optical conversion and multiwavelength laser.

Yuping Chen received the Ph.D. degree in optics from the Department of Physics, Shanghai Jiao Tong University (SJTU), Shanghai, China, in 2002.

From August 2005 to Aug. 2006, she was a Postdoctoral Fellow at the Institute of Optics, University of Rochester, New York. She is currently an Associate Professor with Department of Physics, the State Key Laboratory of Advanced Optical Communication System and Networks, SJTU. She has published over 30 papers in refereed journals and conferences. Her current research interests include quasi-phase-matching nonlinear wavelength conversion, slow and fast light technique and all-optical signal processing.

Mingjun Gong received the B.S. degree from Tongji University, Shanghai, China, in 2008. He is currently working toward the M.S. degree at the Department of Physics, Shanghai Jiao Tong University (SJTU), Shanghai, China.

He is currently with the State Key Laboratory of Advanced Optical Communication System and Networks, SJTU. He is currently engaged in the research and development of all-optical conversion.

Xianfeng Chen received the Ph.D. degree in optics from Shanghai Jiao Tong University, Shanghai, China, in 1997.

He is a Professor of Physics with Shanghai Jiao Tong University, Shanghai, China. He has published more than 40 refereed journal articles. His research interests are in nonlinear optics and nano-photonics, especially quasi-phase-matching nonlinear optics, photonics and devices in magnetic fluid, micro- and sub-micro fiber.